

# Conformal Geometry and the Universe

BY ANTHONY LASENBY

*Astrophysics Group, Cavendish Laboratory, Madingley Road,  
Cambridge CB3 0HE, UK*

The conformal approach to Euclidean geometry introduced by David Hestenes, uses null vectors in an enlarged space to represent points. Here we show how these same techniques can be extended to the curved spacetimes relevant in cosmology. An extended example is given of the transfer of a result from 2d non-Euclidean geometry to 4d de Sitter space (the Origin Lemma in the Poincaré disc), and implications of this conformal approach for asymptotically de Sitter universes, such as the one we appear to live in, are discussed. In a simplified approach, this suggests that our current universe should be approximately spatially flat but with closed spatial sections. This prediction of approximate flatness is achieved without invoking inflation, but needs refining for realistic universe histories.

**Keywords: conformal geometry, geometric algebra, non-Euclidean geometry, de Sitter space, Friedmann-Robertson-Walker models, Cosmic Microwave Background, cosmological constant, twistors**

## 1. Introduction

This paper gives a brief introduction to some recent work on applying the ‘conformal model’ to the Universe. The conformal model for the geometry of Euclidean space was introduced by David Hestenes (Hestenes 2001), and has been discussed further by several authors (see e.g. Lasenby & Lasenby 2000 and Hestenes *et al.* 2000). In Lasenby *et al.* (2003b) and Wareham *et al.* (2003) we have extended this approach to the case of non-Euclidean geometries, both spherical and hyperbolic, and in Lasenby & Lasenby (2003) have shown how even projective geometry, and new hybrid geometries which allow projective transformations within non-Euclidean geometry, can all be expressed in this fashion. The use of a null vector representation was found to bring great benefits both conceptually and computationally.

Here we wish to show how to extend these results from 2d and 3d non-Euclidean geometry to the spacetime case. In particular we look at de Sitter and anti-de Sitter space, and give an extended example of how a key result from non-Euclidean geometry in 2 dimensions, the ‘Origin Lemma’ (see e.g. Brannan *et al.* 1999) can be carried over to de Sitter space, with no change in the algebraic treatment. Then we look at Friedmann-Robertson-Walker (FRW) models. In these cases, one is dealing with spacetimes which do not have a full set of symmetries, and so some of the usual features do not work. Nevertheless, it is useful even here to investigate the conformal approach, since it leads to some surprising and potentially testable conclusions in relation to the cosmological constant and curvature scale of our present universe. It also provides a much simplified way to discuss Penrose and Rindler’s *cosmology twistors* and the *bang* and *crunch* twistors (Arcaute *et al.* 2003). A fuller account of these ideas is in preparation (Lasenby *et al.* 2003a).

## 2. The conformal approach to geometry

The key feature of the conformal method is the representation of points in a space of signature  $(p, q)$  by null vectors in the space  $(p+1, q+1)$ . By employing the machinery of *geometric algebra* to carry out manipulation of the objects in  $(p+1, q+1)$ , geometric relations in  $(p, q)$  can be cast into a ‘covariant’ form, in which rotor transformations in the higher space are all that are required to encode the full group of conformal transformations. All the machinery of incidence relations from projective geometry can now be applied to spheres, circles and hyperbolae, as well as points, lines and planes, giving a real increase in computational power. Details of both this approach and the geometric algebra notation we use are given in Wareham *et al.* (2003) (this volume), and so are not repeated here. A full introduction to geometric algebra, and details of its application in Euclidean and non-Euclidean geometry, is contained in Doran & Lasenby (2003), and much more detail on the covariant approach is contained in Lasenby & Lasenby (2003) and Lasenby *et al.* (2003b). We should also mention the independent work on using Clifford algebra for non-Euclidean geometry carried out by Li *et al.* (see e.g. Li 2001).

## 3. de Sitter space

As a first step, we begin with the simplest case, which is de Sitter space, and examine this via a 6d conformal approach. We know (Lasenby *et al.* 2003b; Doran & Lasenby 2003; Wareham *et al.* 2003) that in order to get 2d or 3d hyperbolic space, we need to keep invariant the vector  $e$ . This suggests that using exactly the same approach for 4d spacetime, we will get de Sitter space, since this has constant negative curvature, just like hyperbolic space. (Note there is a subtlety here, however, in that the spatial sections of de Sitter space correspond to *spherical* rather than hyperbolic geometry. We will see this shortly in terms of the distance function.) To get anti-de Sitter space, which is also important in modern cosmology, one keeps invariant  $\bar{e}$ .

So we have as our basis vectors in the 6d space the usual set for special relativity, supplemented by two extra:

$$e_0, e_1, e_2, e_3, e \text{ and } \bar{e} \quad (3.1)$$

where

$$e_0^2 = 1, \quad e_i^2 = -1 \quad (i = 1, 2, 3), \quad e^2 = 1 \quad \text{and} \quad \bar{e}^2 = -1 \quad (3.2)$$

Let us write  $x$  as the position in 4d spacetime and  $x^2$  as its usual special relativistic length. Specifically, if we use sans serif to indicate the Cartesian components, we have

$$x = x^\mu e_\mu = te_0 + xe_1 + ye_2 + ze_3 \quad \text{and so} \quad x^2 = t^2 - x^2 - y^2 - z^2 \quad (3.3)$$

Our basic representation function is the same null vector as one would use in the Minkowski case, but scaled (in this de Sitter case) to make  $X \cdot e = -1$ , i.e.

$$X = \frac{1}{\lambda^2 - x^2} (x^2 n + 2\lambda x - \lambda^2 \bar{n}) \quad (3.4)$$

where

$$n = e + \bar{e} \quad \text{and} \quad \bar{n} = e - \bar{e} \quad (3.5)$$

Here  $\lambda$  is a constant with the dimensions of length introduced in exactly the same way as in the 2d or 3d cases, in order to make  $X$  dimensionally homogeneous.

We can use exactly the same type of distance function as in the lower dimensional cases, but now have to be careful about signs of intervals. We define

$$d(x, y) = \begin{cases} \lambda \sinh^{-1} \sqrt{-\frac{X \cdot Y}{2}} & \text{if } X \cdot Y \text{ is negative,} \\ 0 & \text{if } X \cdot Y = 0, \\ \lambda \sin^{-1} \sqrt{\frac{X \cdot Y}{2}} & \text{if } X \cdot Y \text{ is positive.} \end{cases} \quad (3.6)$$

To find out what sort of space we have thereby obtained, we can use this distance function to deduce a metric. The relation we need, coming direct from a Taylor expansion, is

$$g_{\mu\nu}(x) = \frac{1}{2} \frac{\partial^2 (d^2(x, y))}{\partial y^\mu \partial y^\nu} \Big|_{y=x} \quad (3.7)$$

Applying this in the current case yields

$$ds^2 = g_{\mu\nu} dx^\mu dx^\nu = \frac{\lambda^4}{(\lambda^2 - x^2)^2} (dt^2 - dx^2 - dy^2 - dz^2) \quad (3.8)$$

which, since this is just the usual special relativistic metric scaled by a position dependent factor, is a conformally flat space, as expected.

Since we have a metric, we can now work out the curvature and geodesic equations in this space. Carrying out the computations required to get the Einstein tensor (not gone through here), we find that in cosmological terms the space corresponds to what one would get with no matter, and a positive cosmological constant  $\Lambda$  related to  $\lambda$  via

$$\Lambda = \frac{12}{\lambda^2} \quad (3.9)$$

Similarly, evaluating the Riemann curvature tensor, we find that the space has a constant, negative, curvature of  $-4/\lambda^2$ .

For the geodesic equations, adopting a standard GR (general relativity) route one finds for the geodesics in e.g. the  $(\mathbf{t}, \mathbf{x})$  plane (taking this as an illustration)

$$\begin{aligned} \ddot{\mathbf{t}} &= \frac{2}{\lambda^2 - x^2} (2 \dot{\mathbf{t}} \dot{\mathbf{x}} - \mathbf{t}(\dot{\mathbf{t}}^2 + \dot{\mathbf{x}}^2)) \\ \ddot{\mathbf{x}} &= \frac{2}{\lambda^2 - x^2} (-2 \dot{\mathbf{t}} \dot{\mathbf{x}} + \mathbf{x}(\dot{\mathbf{t}}^2 + \dot{\mathbf{x}}^2)) \end{aligned} \quad (3.10)$$

where the dots indicate differentiation with respect to the affine parameter along the path. Note this is for particles with mass. For massless particles such as light, the conformal nature of the metric means that they travel along null geodesics which are just lines at  $45^\circ$  in the  $(\mathbf{t}, \mathbf{x})$  plane, precisely as in special relativity.

Integrating these (massive particle) geodesics will clearly run into trouble at  $x^2 = \lambda^2$ . This is a hyperbolic line which we can take as corresponding precisely to the edge of the bounding disc in the Poincaré disc representation of hyperbolic geometry. Here we will call it the ‘boundary hyperbola’. To get a picture of geodesics in de Sitter space, we can radiate geodesics numerically from a point, obtaining the diagram shown in Fig. 1, which also shows both branches of the boundary hyperbola. In this case  $\lambda$  has been chosen as 2 and the point from which the geodesics emanate is  $\mathbf{t} = 1, \mathbf{x} = 0$ .

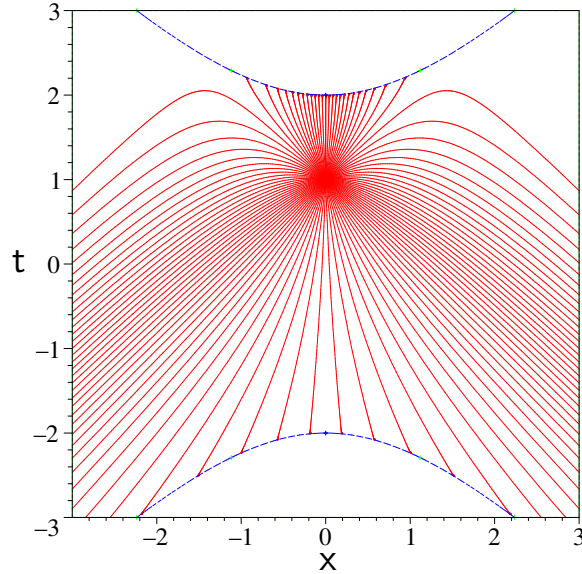


Figure 1. Geodesics in the  $y = 0, z = 0$  plane, emanating from the point  $(t, x) = (0, 1)$  in a de Sitter space with  $\lambda = 2$ . The dashed lines show the position of the boundary hyperbola.

#### 4. Conformal approach to de Sitter space

So far we have been looking at geodesics etc. via differential geometry and the metric. Now we turn to the ‘conformal model’ approach.

To investigate the form of the geodesics, we look at what ‘d-lines’ become in the conformal version of de Sitter space, since we expect these to correspond to the geodesics. To obtain the d-line through points  $A$  and  $B$  we know we should form

$$L = A \wedge B \wedge e \quad (4.1)$$

and that the points lying on the line will be the solutions of  $X \wedge L = 0$ . Carrying this out for points  $a$  and  $b$  lying in the  $(t, x)$  plane, we obtain the following equation for the coordinates of  $x$ :

$$t^2 - x^2 - 2\alpha t - 2\beta x + \lambda^2 = 0 \quad (4.2)$$

where  $\alpha$  and  $\beta$  are functions of the coordinates of  $a$  and  $b$ . This is a hyperbola, as we would expect, and has the special property that it intersects the boundary hyperbola,  $t^2 - x^2 = \lambda^2$  at ‘right angles’, as shown in Fig. 2. (It may not look as though the intersection is perpendicular in the diagram, but this is because the orthogonality is with respect to the Lorentz metric applicable locally at each point, and not the Euclidean geometry in which we have drawn the diagram.)

To prove that the intersection really is perpendicular, we can take the special case of a particle at rest at the origin, and then transform this to the general case via a combined translation/rotation rotor. (Note rotations in e.g. the  $(t, x)$  plane are *Lorentz boosts*, while those involving only spatial directions are ordinary rotations.)

The rotors which carry out translations are of the form

$$T = \frac{1}{\sqrt{\lambda^2 - a^2}} (\lambda + \bar{e}a) \quad (4.3)$$

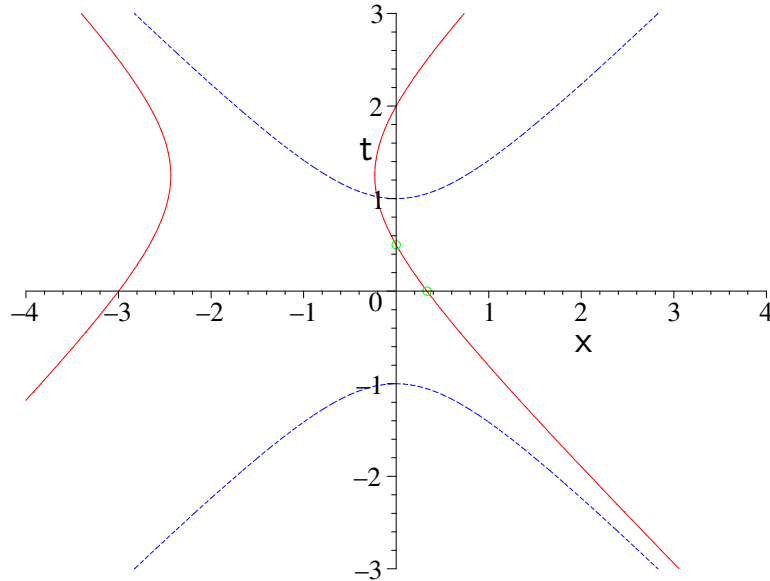


Figure 2. A d-line in the  $y = 0, z = 0$  plane, passing through the points  $(t, x) = (0, 1/3)$  and  $(1/2, 0)$  in a de Sitter space with  $\lambda = 1$ . The solid lines show the full set of solutions of the equation  $X \wedge L = 0$  while the dashed lines show the position of the boundary hyperbola.

where  $a$  is the 4-d spacetime vector through which we wish to translate. Now the time axis,  $x = 0$ , is clearly a d-line, and this intersects the boundary hyperbola at right angles (both in a Euclidean and Lorentzian sense). Conformal transformations preserve angles, hence by moving this d-line around with the above rotor, we recover the whole set of d-lines which intersect the boundary hyperbola (some are shown in Fig. 3) and for all of them we can deduce the boundary hyperbola crossing is perpendicular.

### 5. The ‘Origin Lemma’ in the Poincaré disc

To illustrate more features of the geometry, we take a theorem from the Poincaré disc case, the ‘Origin Lemma’ on p268 of Brannan, Esplen & Gray (1999), and then in the next section demonstrate its equivalent in de Sitter space.

The *Origin Lemma* is the following:

**Lemma 5.1 (Origin Lemma).** *Let  $A$  be a point on the Poincaré disc other than the origin  $O$ . Then there exists a d-line  $\ell$  such that non-Euclidean reflection in  $\ell$  maps  $A$  to  $O$*

This setup is illustrated in in Fig. 4. Here  $\ell$  is the desired d-line,  $P$  and  $Q$  are its intersection points with the bounding circle, and  $R$  its Euclidean centre. One of the things which Brannan *et al.* prove in the course of proving the Origin Lemma is that  $R$  can be found by inverting the point  $A$  in the boundary circle, which they call ‘an unexpectedly memorable result’.

We now see how we would go about establishing this Lemma in our usual non-Euclidean setup. We shall phrase our discussion in 2d, but it obviously extends to 3d etc. as well. We begin with a theorem.

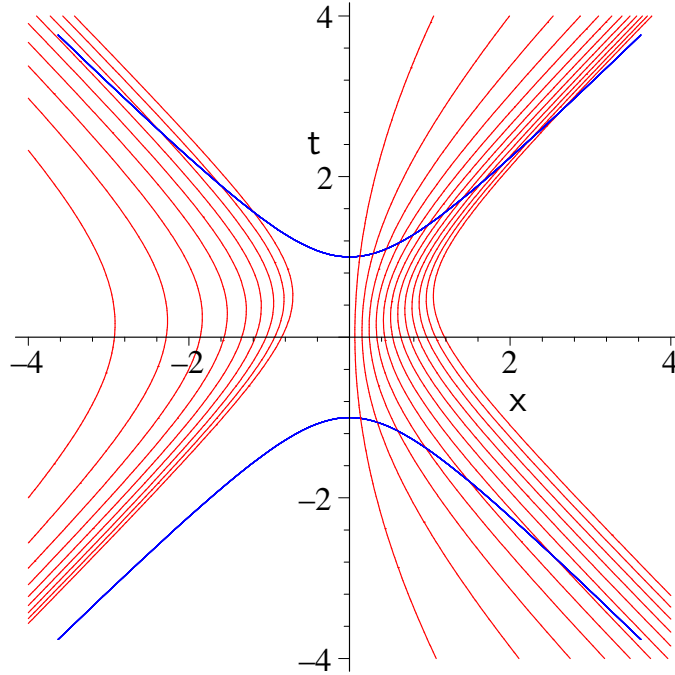


Figure 3. Some d-lines in de Sitter space obtained by using a translation rotor to displace the  $t$  axis to the right and upwards. Equal increments along a direction  $(0.27, 0.55)$  in  $(t, x)$  space are shown. Initially the other branches of the hyperbolae are not visible, but then start entering at the left.

**Theorem 5.2.** *Given two points  $A$  and  $B$ , then*

- (i)  $L = I(A - B)$  is a d-line;
- (ii) The non-Euclidean reflection of  $A$  in  $L$  is  $B$ .

**Proof:** (i) A d-line is a grade-3 object of the form  $e \wedge A_2$  where  $A_2$  is a grade-2 blade. Thus a blade  $L$  of grade 3 is a d-line  $\Leftrightarrow L \wedge e = 0$ . Now

$$[I(A - B)] \wedge e = I[(A - B) \cdot e] = 0 \quad (5.1)$$

since  $X \cdot e = -1$  for any point  $X$ ; thus indeed  $L = I(A - B)$  is a d-line.

- (ii) The non-Euclidean reflection of a point  $A$  in a line  $L$  is  $LAL$ . (Note in our setup, we could take this as a definition of what is meant by non-Euclidean reflection. However, we could also note that in Brannan *et al.* non-Euclidean reflection is defined as inversion in the Euclidean circle of which the d-line is a part, and this coincides with our definition up to scale.) This is properly normalized if  $L$  is, i.e. if  $L^2 = 1$ , then it follows that  $(LAL) \cdot e = -1$ . A normalized version of  $I(A - B)$  is given by

$$L = \frac{\sqrt{(\lambda^2 - a^2)(\lambda^2 - b^2)}}{2\lambda|a - b|} I(A - B) \quad (5.2)$$

Applying this to  $A$ , we find (by straightforward computation) that  $LAL = B$ , proving what we wanted. Interchanging the roles of  $A$  and  $B$  it follows that  $LBL = A$ , i.e. that the non-Euclidean reflection of  $B$  in  $L$  is  $A$ .

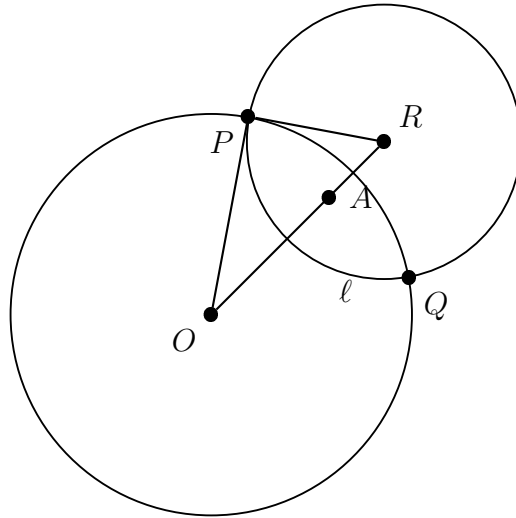


Figure 4. The ‘Origin Lemma’ in the Poincaré disc.

We now see that what we have proved is in fact a generalization of the Origin Lemma, since we have proved that for any two points  $A$  and  $B$  in the Poincaré disc there is a d-line in which each is the non-Euclidean reflection of the other — we just take the d-line given by Eq. 5.2. The Origin Lemma as stated is then just the special case  $B = -\bar{n}$ , for which  $L = \sqrt{\lambda^2 - a^2}/(2a) I(A + \bar{n})$ .

The additional result commented on by Brannan *et al.* — namely that the centre of the non-Euclidean circle of which the d-line is a part, is given by inverting  $A$  in the bounding circle — is easy to establish also. We first need the result:

**Lemma 5.3.** *If the trivector  $L$  represents a d-line then it is invariant under inversion in the bounding circle.*

To prove this, it is convenient first of all to establish the way in which points on the bounding circle are represented. Consider  $X = F(x)$  for a point  $x$  given by  $x = (\lambda - \delta)(\cos \phi e_1 + \sin \phi e_2)$ . Then as  $\delta \rightarrow 0$ , one finds that to lowest order,  $X \rightarrow \lambda(\cos \phi e_1 + \sin \phi e_2 + \bar{e}) \delta^{-1}$ . This means that boundary points have to be represented differently from the interior points, which makes sense since they are not part of the ‘universe’ represented by the disc interior, but that a convenient way of doing this is to take this limiting form times  $\delta$ , i.e. for the boundary point at angle  $\phi$  we take:

$$X = \lambda(\cos \phi e_1 + \sin \phi e_2 + \bar{e}) \quad (5.3)$$

This is a null vector, with the right dimensions, and can be moved around by rotors just as for the interior points. It coincides with the representation of interior points up to scale (here infinite!), and so can be used in incidence relations with points elsewhere in the disc. With this, we can now prove our lemma.

**Proof of Lemma 5.3:** Consider the d-line  $\ell$  shown in Fig. 4. This intersects the bounding circle at the points  $P$  and  $Q$ . The d-line  $\ell$  can therefore be written, up to scale as

$$L = P \wedge Q \wedge e \quad (5.4)$$

Now because any bounding circle point does not contain  $e$  (see equation 5.3), we have  $ePe = -P$  and  $eQe = -Q$ . Thus the inversion of  $L$  in the bounding circle,  $eLe$ , is equal to  $L$  as claimed.

We can now use this result to show that the Euclidean centre of  $\ell$  is the inverse of  $A$  in the bounding circle. We know already that  $\ell$  is represented, up to scale, by  $L = I(A + \bar{n})$ . Thus

$$eLe = L = -I(eAe + n) \quad (5.5)$$

Up to scale we can therefore write the dual of  $L$  as  $-eAe - n$ , which is of the form of a null vector minus a positive multiple of  $n$ . The null vector involved,  $-eAe$ , must therefore be the centre of  $L$  when viewed as a Euclidean circle, which proves what we need. (This also suggests that outside the boundary circle, our normalisation should be  $X \cdot e = 1$ , instead of  $-1$ , but we will not pursue this further here.)

As a final point, though not relevant to the ‘intrinsic’ picture in non-Euclidean space, we note that it appears plausible from Fig. 4 that  $P$ ,  $Q$  and  $A$  lie on a straight line. It is interesting to see how to prove this algebraically.

First, given a d-line  $L$ , we can find where it intersects with the boundary circle via just dotting with  $e$ . E.g. if  $L = P \wedge Q \wedge e$  as above, then since neither  $P$  or  $Q$  contains  $e$ , it is clear that  $P \wedge Q = L \cdot e$ .  $P$  and  $Q$  can then be recovered individually in the usual way, if we need to find them.

However, here, we just need to show that  $P \wedge Q \wedge A \wedge n = 0$ , in order to demonstrate that  $P$ ,  $Q$  and  $A$  lie on a straight line. Since (up to scale) we also have  $L = I(A + \bar{n})$ , we can see that the result we want follows if

$$[(A + \bar{n}) \wedge e] \cdot [A \wedge n] = 0 \quad (5.6)$$

But this follows since

$$\begin{aligned} [(A + \bar{n}) \wedge e] \cdot [A \wedge n] &= [(A + e - \bar{e}) \wedge e] \cdot [A \wedge (e + \bar{e})] \\ &= (A - \bar{e}) \cdot (e + \bar{e}) A \cdot e - (A - \bar{e}) \cdot A e \cdot (e + \bar{e}) \\ &= -(A \cdot e + A \cdot \bar{e} + 1) + A \cdot \bar{e} \end{aligned} \quad (5.7)$$

which is indeed zero.

## 6. The Origin Lemma in de Sitter space

In transferring to de Sitter space, we need no new work algebraically — it is just a matter of finding out where the various points lie. We will work as above in the  $(t, x)$  plane. The only actual algebraic change is for the boundary points. These will now be of the form

$$X = \lambda(\cosh \phi e_0 + \sinh \phi e_1 + \bar{e}) \quad (6.1)$$

However, again no change in working is entailed, since these also have the key feature of containing no  $e$  component, which was all we needed above.

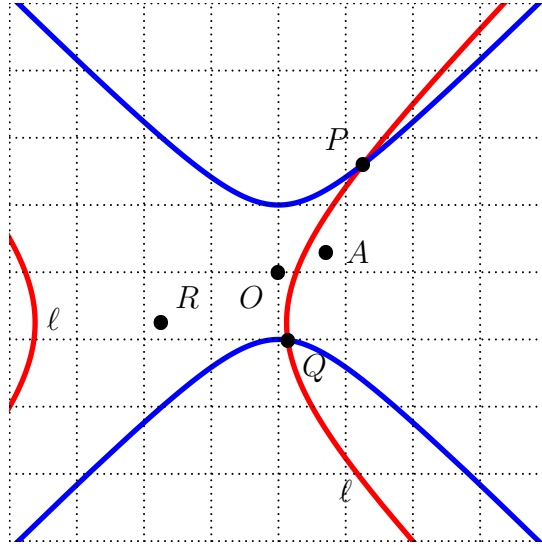


Figure 5. The ‘Origin Lemma’ in de Sitter space — spacelike case.

There are two distinct cases to examine for the Origin Lemma in de Sitter space, corresponding to whether the point  $A$  lies at a spacelike or timelike separation from the origin  $O$ . Which of these is the case is easy to establish, since as noted above, the null rays in de Sitter space all go at  $45^\circ$  in our conformal representation, and hence we just have to see whether the Euclidean line from  $O$  to  $A$  lies at an angle less than or greater than  $45^\circ$  as measured from the  $x$  axis.

We first consider the spacelike case, which is illustrated in Fig. 5. We see in this figure similar features to the example from non-Euclidean space, and it can be interpreted similarly. The line  $\ell$  is such that ‘non-Euclidean’ reflection of  $A$  in  $\ell$  yields  $O$ , and its representation  $L$  is proportional to  $I(A+\bar{n})$ . The Euclidean ‘centre’ of this hyperbola, namely where its asymptotes intersect, is marked  $R$ , and as in the non-Euclidean case corresponds to the point inverse to  $A$ , i.e. to  $eAe$ . Note that the inversion here is of a spacelike point, and so corresponds to the sort of inversion that occurs in *spherical* rather than hyperbolic geometry. Thus it flips sign to end up at the other side of the origin. The points  $P$  and  $Q$  mark the intersection of  $\ell$  with the bounding hyperbola, and we again see that  $P$ ,  $Q$  and  $A$  lie on a Euclidean straight line. As before we can find  $P$  and  $Q$  individually by taking  $F = L \cdot e$ , and then after normalising this, i.e. rescaling so that  $F^2 = 1$ , we form the projectors

$$\Theta = \frac{1}{2}(1 + F), \quad \tilde{\Theta} = \frac{1}{2}(1 - F) \quad (6.2)$$

Now, up to scale  $F = P \wedge Q$  and  $P$  and  $Q$  are correctly normalised boundary points. Hence  $F \cdot \bar{e} \propto P - Q$ , and we derive

$$P = -\tilde{\Theta}(F \cdot \bar{e}) \quad \text{and} \quad Q = \Theta(F \cdot \bar{e}) \quad (6.3)$$

In Fig. 6 we show what happens for a *timelike* separation of  $A$  and  $O$ . This time,  $\ell$  does not intersect the boundary hyperbola at all, so  $P$  and  $Q$  cannot be defined. Algebraically this corresponds to the fact that  $F = L \cdot e$  has negative square in this

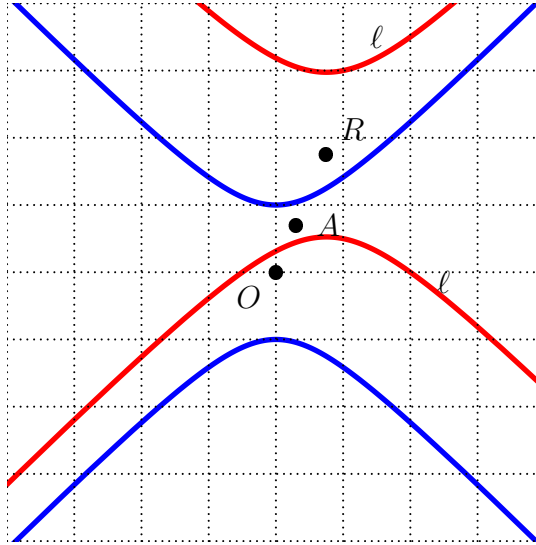


Figure 6. The ‘Origin Lemma’ in de Sitter space — timelike case.

case. Otherwise, however, the same features as in the preceding cases can be seen, in particular that the ‘Euclidean centre’ of the d-line lies at the inverse point of  $A$  with respect to the boundary.

## 7. The infinity twistors of Penrose and Rindler

In Penrose & Rindler (1986), Section 9.5, valence-two *infinity* twistors  $\mathbf{I}_{\alpha\beta}$  are introduced. There is one for each of de Sitter, anti-de Sitter and ordinary Minkowski space. A feature of their defining properties is that their contraction with the valence-two twistor  $\mathbf{R}_{\alpha\beta}$ , which represents position in 4-d space, is constant. In Arcaute, Lasenby & Doran (2003), it is shown how valence-1 twistors can be represented by a particular type of Dirac spinor in the GA approach, and hence how valence-2 twistors correspond to 2-particle Dirac spinors, which are most easily represented in the Multiparticle Spacetime Algebra (MSTA) (see also Lasenby & Lasenby 2001). The translation of the infinity twistors then turn out to correspond to particular types of relativistic singlets in 2-particle quantum mechanics. Conformal transformations then have their counterpart in operations on 2-particle states. For example, *inversion* in 4d spacetime becomes the operation of swapping the spin states (up  $\leftrightarrow$  down) of the two particles (see Arcaute *et al.* 2003; Lasenby & Lasenby 2001).

This is interesting, but for present purposes the most interesting aspect is how this relates to our ‘single particle’ 6-dimensional representation of spacetime. This is also discussed in the above papers, with the conclusion that  $\mathbf{I}_{\alpha\beta}$  corresponds to  $e$  in the de Sitter case,  $\bar{e}$  for anti-de Sitter space and  $n$  for Minkowski space. The Penrose and Rindler relation  $\mathbf{I}_{\alpha\beta}\mathbf{R}^{\alpha\beta} = 2$  is then just a restatement of the covariant relations that  $X \cdot e$ ,  $X \cdot \bar{e}$  and  $X \cdot n$ , respectively, are equal to  $-1$  for properly scaled null vectors  $X$ .

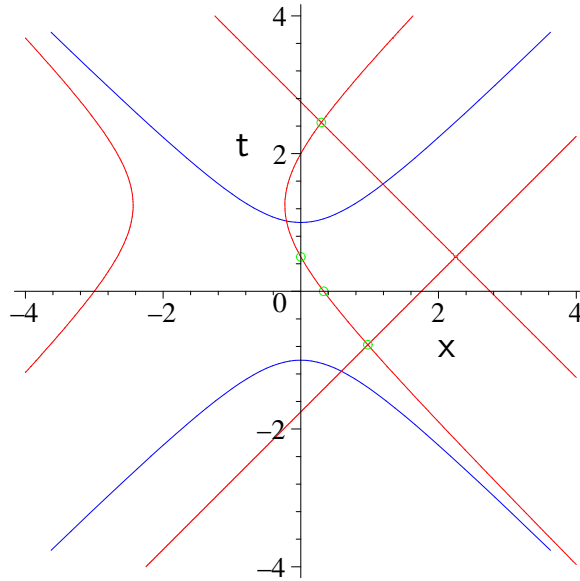


Figure 7. The same d-line through the points  $(t, x) = (0, 1/3)$  and  $(1/2, 0)$  is shown as in Fig.2. Also shown here are the intersections with the light cone through the point  $(t, x) = (9/4, 1/2)$ , found using the method described in the text.

The twistor approach thus encodes some features of the conformal approach to spacetime that we have been discussing so far. What seems to be quite new in our conformal approach, however, is the ability to link geometric objects such as spheres, lines, planes and hyperboloids, with algebraic objects of a given grade, and manipulate them covariantly, as we have illustrated with the Origin Lemma. Moreover, the null-vector conformal approach seems very much simpler than the machinery which is required for twistors, and links with virtually no change to the 2d and 3d Euclidean cases.

## 8. Null cone structure and event horizons

So far, not much has been said about the properties of light paths, other than that they run at  $\pm 45^\circ$  in our conformal diagrams. We shall now demonstrate that the null vector conformal approach is useful in providing us with novel tools for dealing with light paths, and their interaction with geodesics of massive particles (the ‘d-lines’). Again, this seems to go beyond anything that is available using the twistor approach.

The first thing to note is that the light cone emanating from a point  $P$  is represented by the object  $IP$ . This is because

$$X \wedge (IP) = 0 \implies X \cdot P = 0 \quad (8.1)$$

and the latter equation is satisfied by those points that are a zero distance from  $P$ , i.e. precisely those points  $X$  lying on the light cone of  $P$ .

Since we have an object to represent the light cone, we can take its intersection with other objects in the usual way. As an illustration, we show in Fig. 7 the intersections of the light cone through the point  $(t, x) = (9/4, 1/2)$  with the d-line

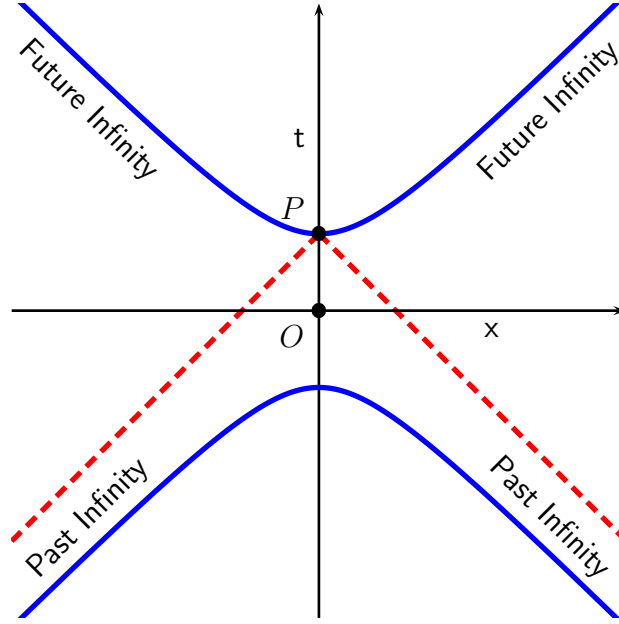


Figure 8. The event horizon (dashed lines) for an observer travelling up the  $t$  axis in de Sitter space. The event horizon is represented by the object  $IP$ , where  $P = \lambda(e_0 + \bar{e})$ .

$L$  which runs through the points  $(t, x) = (0, 1/3)$  and  $(1/2, 0)$ . We can intersect the d-line with the light cone by forming  $F = L \cdot P$ . If the two intersection points are given by  $A$  and  $B$ , then  $F$  will be proportional to  $A \wedge B$ .  $A$  and  $B$  are regular interior points satisfying  $A \cdot e = -1$  and  $B \cdot e = -1$ . Thus  $F \cdot e$  will be proportional to  $A - B$ . By forming the projectors  $\Theta$  and  $\tilde{\Theta}$  as in equation (6.2), we can then recover  $A$  and  $B$  individually via (e.g.)

$$A = -\tilde{\Theta}(F \cdot e) \quad \text{and} \quad B = \Theta(F \cdot e) \quad (8.2)$$

Following this procedure then yields the points as shown in the figure. This assumes that  $F = L \cdot P$  is normalizable, i.e. that we can rescale  $F$  so that  $F^2 = 1$ . But we will always be able to do this provided that the geodesic does actually intersect the light cone. If it does not, then we will find  $F^2 < 0$ , and if it just touches, then  $F^2 = 0$ .

So far we have discussed light cones for interior points — the light cones for boundary points are also very important however. Consider the point where the positive  $t$  axis intersects the boundary hyperbola. The backward light cone from this point must be the ‘event horizon’ for the particular observer who follows the geodesic which travels up the  $t$  axis in de Sitter space. This is because an event horizon for a given observer is defined as the set of points exterior to which any signals which are emitted do not arrive at the observer even after infinite proper time. (This might more properly perhaps be called a ‘cosmological horizon’, since it depends on the observer, but the name ‘event horizon’ is often used.) In Fig. 8 we show this basic setup. Only signals emitted within the cone-shaped region enclosed by the dashed lines will be able to reach the observer before infinite proper time

is reached, which is the point  $P$  where the observer's geodesic, the upward  $t$  axis, intersects the boundary hyperbola. The event horizon is therefore represented as an object by  $IP$ , where  $P = \lambda(e_0 + \bar{e})$  is the boundary point, and we can find its intersection with geodesics etc. as above.

By Lorentz rotating, or by translation, we can find the event horizon for an observer on any other geodesic that we wish. It will always consist of backward lightcones from points on the 'future infinity' boundary.

## 9. The Universe

A notable feature of the actual universe is that it is evolving in time, and in particular seems to have had a big bang origin. Since both de Sitter and anti-de Sitter space are strictly homogeneous, both in time and space, this means that we have to break this homogeneity in order to begin representing the real universe using the conformal model approach.

This is discussed in the context of twistor representations in Penrose & Rindler. They define *Bang* and *Crunch* twistors, which allow one to specify at what time points the big bang, and in the case of collapsing universes, the big crunch, occur. These twistors are quite complicated objects, but on translation into our 6d conformal model, become very simple. E.g. the big bang becomes just the point where  $X \cdot e_0 = 0$ , and in fact the 4d vector  $e_0$  is the complete translation for the Bang twistor.

We now discuss some aspects of the 6d conformal approach representation for the Friedmann-Robertson-Walker (FRW) models. Further details are given in Lasenby *et al.* (2003a). We need to consider dot products of our null vector representative  $X$  with each of  $e_0$ ,  $n$ ,  $e$  and  $\bar{e}$ . Thus we use a single unscaled null vector

$$X = x^2 n + 2\lambda x - \lambda^2 \bar{n} \tag{9.1}$$

to express the conformal factors. We define the latter via

$$\bar{h}(a) = f(x)a \tag{9.2}$$

where  $f(x)$  is a dimensionless scalar function of position, and  $a$  is a general 4d vector. Here we are using the Gauge Theory Gravity (see Lasenby *et al.* 1998) way of defining the metric. This works with a linear function  $\bar{h}$ , which is effectively the *square root* of the metric used in general relativity. We will not explore further this distinction here, except to note that the sign of  $f$  may be important, and that information about it is preserved in the GTG approach, whereas it is lost in GR. The corresponding GR metric is

$$ds^2 = \frac{1}{f^2} (dt^2 - dx^2 - dy^2 - dz^2) \tag{9.3}$$

The types of universes which can be considered are shown in the left hand column of Table 1. Our emphasis is on those which have a non-zero cosmological constant,  $\Lambda$ . The current cosmological data strongly support the view that the universe began with a big bang, but also that it is now tending towards domination by a positive  $\Lambda$ , and is therefore entering an *asymptotic de Sitter* stage.

Table 1. *Conformal model representations of big-bang models*

Model	Conformal representation
Flat, no $\Lambda$ , dust (Einstein-de Sitter):	$f = \left(\frac{\lambda}{t}\right)^2 = \left(\frac{X \cdot n}{X \cdot e_0}\right)^2$
Flat, with $\Lambda$ ( $g$ an elliptic function):	$f = g\left(\frac{t}{\lambda}\right) = g\left(\frac{X \cdot e_0}{X \cdot n}\right)$
de Sitter (i.e. no matter, just $\Lambda$ ):	$f = 2\frac{X \cdot e}{X \cdot n}$
Anti-de Sitter (no matter, negative $\Lambda$ ):	$f = 2\frac{X \cdot \bar{e}}{X \cdot n}$
Hyperbolic spatial sections, with $\Lambda$ (open):	$f = g\left(\frac{X \cdot e_0}{X \cdot \bar{e}}\right) \frac{X \cdot e_0}{X \cdot n}$
Spherical spatial sections, with $\Lambda$ (closed):	$f = g\left(\frac{X \cdot e_0}{X \cdot e}\right) \frac{X \cdot e_0}{X \cdot n}$

This current data (mainly distant Supernovae and the Cosmic Microwave Background, see e.g. Perlmutter *et al.* 1999 and Lasenby 2002) also strongly suggest that the universe is close to being *spatially flat*, i.e. that

$$\Omega_{\text{tot}} \equiv \Omega_m + \Omega_\Lambda \approx 1 \quad (9.4)$$

where  $\Omega_m$  is the matter density (dark plus ordinary) divided by the critical density,  $3H_0^2/(8\pi G)$ , and  $\Omega_\Lambda \equiv \Lambda/(3H_0^2)$ . The precise degree of flatness is not yet clear however, since what is deduced from the data depends on several assumptions about the early universe, and so it is still useful to consider general non-flat models, where  $\Omega_m + \Omega_\Lambda$  is not precisely 1.

The right hand column of Table 1 shows what values of  $f$  are required for each of the models considered, written in a form which emphasizes the role of the null vector  $X$ . Thus, for example, we already know by comparing equation (3.8) with equation (9.3) that

$$f = \frac{\lambda^2 - x^2}{\lambda^2} \quad (9.5)$$

gives us the de Sitter space metric. We now employ the null vector representation by noting that this same  $f$  can be written as

$$f = 2\frac{X \cdot e}{X \cdot n} \quad (9.6)$$

The other entries are arrived at similarly (details are given in Lasenby *et al.* 2003a). We see that universes with a big bang origin all involve the combination  $X \cdot e_0$ . Those universes with hyperbolic spatial sections involve  $X \cdot \bar{e}$  and those with spherical spatial sections involve  $X \cdot e$ . All of them involve the combination  $X \cdot n$ , which is effectively the rescaling required in order for the result to be portrayed in ordinary Lorentzian space. (This latter aspect is discussed in a Euclidean context in Doran & Lasenby 2003.) Because of the explicit  $e_0$  in the other universes, only the de Sitter and anti-de Sitter universe are fully ‘covariant’, although one can navigate through the spatial hypersurfaces of all of them using rotors of course.

The entries in Table 1 form one of the main results of this paper. From them, by visual inspection, a rather surprising conclusion starts to emerge. As stated above,

cosmological observations suggest that we live in a universe which has a significant amount of matter currently, but will ultimately approach a de Sitter state. The conformal representation we would like to employ, in terms of the null vector  $X$ , should therefore asymptotically approach the de Sitter form. However, the flat  $\Lambda$  universe, usually considered as the most likely to be a good representation of our actual universe, fails to make the transition to an ultimate de Sitter state in the expected way. This is clear from the fact that whatever the function  $g$  in

$$f = g\left(\frac{\mathbf{t}}{\lambda}\right) = g\left(\frac{X \cdot e_0}{X \cdot n}\right) \quad (9.7)$$

(in fact it is an elliptic function), the function  $f$  cannot tend to the form  $2X \cdot e/X \cdot n$ , since the argument of  $g$  always involves  $X \cdot e_0$ . What is happening is that the conformal representation of flat  $\Lambda$  models effectively picks out different spatial hypersurfaces from those involved in representing the de Sitter model.

If we look at the list of  $X$ -vector representations, we see that the only model which has the possibility of behaving as we would wish, is the  $\Lambda$  model with spherical spatial sections. This has

$$f = g\left(\frac{X \cdot e_0}{X \cdot e}\right) \frac{X \cdot e_0}{X \cdot n} \quad (9.8)$$

Writing  $\chi \equiv -X \cdot e_0/X \cdot e$  (the minus sign to make  $\chi$  positive) we can see that such a universe will end up in our conformal version of de Sitter provided

$$g(\chi) \propto \frac{1}{\chi} \quad \text{for large } \chi \quad (9.9)$$

since then the  $X \cdot e_0$ 's can cancel, to leave us with the right quantity.

To check whether  $g(\chi) \propto 1/\chi$  holds, we need to integrate the differential equation satisfied by  $g$ . All the gravitational field equations reduce to this one equation and by using  $\lambda$  to scale out lengths and times, we can reduce this to a first order equation in dimensionless variables (see Lasenby *et al.* 2003a for details).

It turns out the the behaviour of this equation is controlled by a single dimensionless parameter

$$\alpha \equiv \Lambda \lambda^2 \quad (9.10)$$

and in terms of this parameter something remarkable then happens! We find that we have effectively got an eigenvalue problem for the correct behaviour of the universe at (timelike!) infinity. A critical value,  $\alpha_{\text{crit}} \approx 121$  is picked out (see Fig. 9(a)), and this in turn implies a particular relation between curvature and  $\Lambda$ . Using this relation, one can find  $\Omega_m$  from knowledge of  $\Omega_\Lambda$  at any given epoch, and *vice versa*.

Now the current best estimates of  $\Omega_m$ , independent of other parameters, come from surveys of large scale structure in the universe, such as the 2dF redshift survey (Percival *et al.* 2001). These yield  $\Omega_m \sim 0.3$ . In this case the particular value of  $\Omega_\Lambda$  picked out by the requirement that  $g(\chi) \propto 1/\chi$  for large  $\chi$  is  $\Omega_\Lambda \sim 0.8$ . This point in  $(\Omega_m, \Omega_\Lambda)$  space is shown in Fig. 9(b) in relation to recent constraints on these parameters from the supernovae and CMB observations referred to above. One can see that the universe being closed at the 10% level as predicted from our conformal approach, is not incompatible with either data set individually, but is

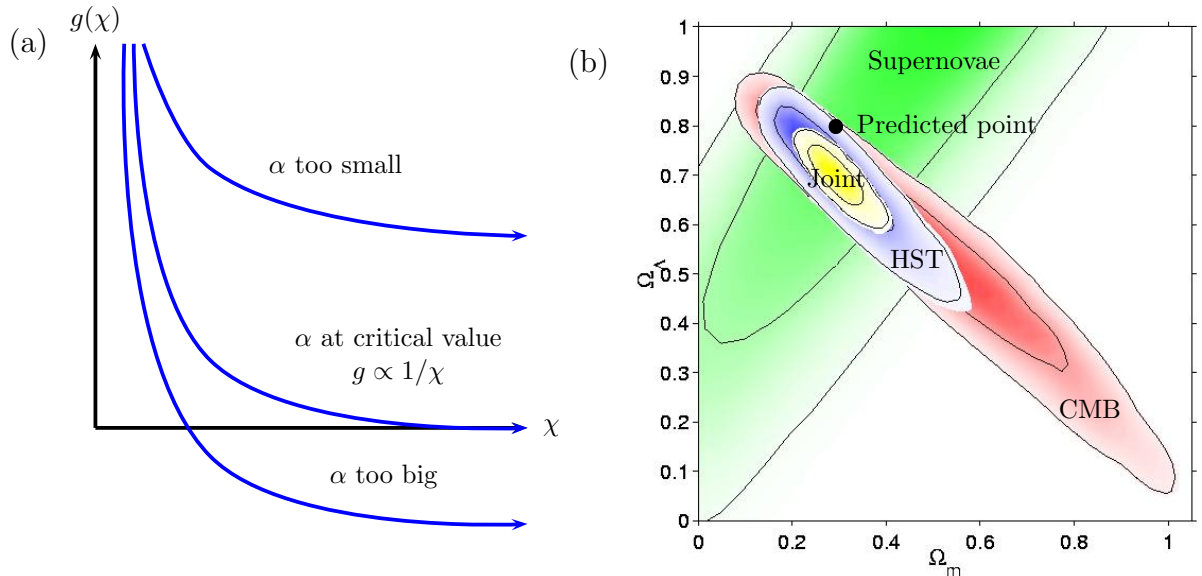


Figure 9. (a) Schematic plots of the function  $g(\chi)$  for a universe containing both  $\Lambda$  and matter, with spherical spatial sections. A critical value of the dimensionless quantity  $\alpha = \Lambda\lambda^2$  is picked out for which  $g(\chi) \propto 1/\chi$  for large  $\chi$ . (b) A plot of recent constraints on  $\Omega_m$  and  $\Omega_\Lambda$  adapted from Lewis & Bridle (2002). 1 and 2  $\sigma$  contours are shown for Type Ia supernovae (Perlmutter *et al.* 1999), labelled SN, Cosmic Microwave Background data, labelled CMB, and from the Hubble Space Telescope Key Project value for  $H_0$  (Freedman *et al.* 2001), labelled HST. The combination of all constraints is marked ‘Joint’. The point predicted on the basis of the conformal approach, assuming  $\Omega_m = 0.3$ , is also shown.

close to being ruled out by their combination. Improved CMB constraints expected in the near future (e.g. from the MAP satellite), will probably provide a definitive resolution of this, and indeed a recent analysis (Slosar *et al.* 2002) of a combination of CMB, supernovae and large scale structure data appears to limit the departure of the universe from flatness to just 3%.

What then are we to make of the apparent result we have obtained from the application of the conformal model approach to the universe? The first thing to say is that it is clearly an interesting attempt, even if this naive application of it is ruled out by the data. Simply by asking that our description in terms of dot products with a 6d null vector  $X$  should yield a particular limit at late times, agreeing with our preferred representation of a de Sitter universe, we have found a physically testable constraint on  $\Omega_m$  and  $\Omega_\Lambda$ . The fact that it is physically testable means that it must translate into a physical requirement in the conventional approach as well, and in Lasenby *et al.* (2003a) a discussion is given in terms of the horizon properties of an asymptotically de Sitter universe.

Secondly, it is remarkable that a universe close to flat is picked out by a requirement that has nothing to do with inflation. Inflation is an exponential expansion in the early universe, driven by the stress-energy tensor of a scalar field, and is able to drive the universe close to flatness, say to 1 part in  $10^{60}$ , at very early times, which is usually supposed to be what is required in order to get  $\Omega_{\text{tot}}$  close to 1 today (see

e.g. Liddle & Lyth 2000). Here, however, we have a universe close to flat picked out by an eigenvalue requirement on the behaviour of the universe at late times. Inflation also solves other problems as well of course, such as the generation of the perturbations needed to form large scale structure in the universe, so the proposal made here is not meant in any way to say that we do not need inflation, merely that the so called ‘flatness problem’ might be susceptible to a different resolution.

Thirdly, we have so far applied the conformal approach only to a very simplified version of the universe. In particular, the matter content has been taken as being dust (i.e pressureless matter) only, whereas we know we should consider also radiation as well (the CMB), which is dynamically important at earlier times. Finally, if there is indeed a period of inflation at very early times, driven by a scalar field, then this should be folded into the model as well, since it would profoundly alter the time development of the function  $g$ . Thus different results can be expected in these cases, and this is under active investigation.

A more basic question is why it should be thought that nature ‘knows about’ the conformal model as we have described it, and seeks to choose the parameters of the universe such that the null-vector conformal representation should be valid until arbitrarily late times. This is clearly a difficult question, but an intriguing possibility is that a link exists with ‘braneworld’ models of the universe (e.g. Randall & Sundrum 1999), in which gravity is a dynamic entity in a higher-dimensional space. To make concrete such a link, would entail enlarging the gauge theory gravity approach (Lasenby *et al.* 1998) to the conformal case, and letting translations be carried out by rotors in 6d space rather than diffeomorphisms in 4d. This is an exciting possibility which is worth pursuing.

## 10. Conclusions

The conformal model approach gives a simple approach to the universe with interesting consequences. A preliminary prediction has been made of a universe closed at about the 10% level, which is probably now incompatible with the current observations, but there is certainly a need to examine more complicated time histories as regards the universe’s matter/field content.

A further point worth noting is that the dimensionful  $\lambda$  we have to introduce in 2d and 3d geometry to make the null vector representation homogeneous, is what sets the scale/age of the universe in 4d. For example, if the universe is indeed in the state discussed above, then taking the Hubble constant as  $H_0 \sim 65 \text{ km s}^{-1} \text{ Mpc}^{-1}$  (Slosar *et al.* 2002), then one can deduce  $\lambda$ , obtaining

$$\lambda \sim 1.01 \times 10^{27} \text{ m} \sim 33 \text{ Gpc} \quad (10.1)$$

This amounts to more than just deducing a length scale from the cosmological constant, which has of course been done many times before, since here it gives the curvature scale as well. It is certainly interesting to speculate about whether this length scale has any fundamental significance.

## Acknowledgements

I would like to thank my collaborators Elsa Arcaute, Chris Doran and Joan Lasenby.

## References

- Arcaute E., Lasenby A., Doran C., 2003, *Twistors and Geometric Algebra*, To be submitted to *J.Math.Phys.*
- Brannan D., Esplen M., Gray J., 1999, *Geometry*. Cambridge University Press
- Doran C., Lasenby A., 2003, *Physical applications of Geometric Algebra*. Cambridge University Press
- Freedman W., *et al.*, 2001, *Astrophys.J.*, **553**, 47
- Hestenes D., 2001, in Bayro-Corrochano E., Sobczyk G., eds, *Geometric Algebra with Applications in Science and Engineering*. Birkauer, Boston, p. 3
- Hestenes D., Li H., Rockwood A., 2000, in Sommer G., ed., *Geometric Computing with Clifford Algebra*. Springer, Heidelberg, p. 3
- Lasenby A., 2002, *Class.Quant.Grav.*, **19**, 3469
- Lasenby A., Doran C., Arcaute E., 2003a, *Conformal representation of asymptotically de Sitter universes*, To be submitted to *Mon.Not.R.astr.Soc.*
- Lasenby A., Doran C., Gull S., 1998, *Phil. Trans. R. Soc. Lond. A*, **356**, 487
- Lasenby A., Lasenby J., 2000, in Cipolla R., Martin R., eds, *The Mathematics of Surfaces IX, Proceedings of The Ninth IMA Conference on the Mathematics of Surfaces, Cambridge, U.K.*. Springer-Verlag, p. 144
- Lasenby A., Lasenby J., 2001, in Bayro-Corrochano E., Sobczyk G., eds, *Geometric Algebra with Applications in Science and Engineering*. Birkauer, Boston, p. 430
- Lasenby A., Lasenby J., 2003, *A covariant approach to geometry*, Submitted to *Proceedings of the 6th Conference on Clifford Algebras and their Applications in Mathematical Physics*
- Lasenby A., Lasenby J., Wareham R., 2003b, *A covariant approach to geometry and its applications in computer graphics*, Submitted to *ACM Transactions on Computer Graphics*
- Lewis A., Bridle S., 2002, *Phys.Rev.D.*, **66**, 103511
- Li H., 2001, *Int.J.Theor.Phys.*, **40**, 81
- Liddle A. R., Lyth D. H., 2000, *Cosmological Inflation and Large-Scale Structure*. Cambridge University Press
- Penrose R., Rindler W., 1986, *Spinors and space-time, Volume II: spinor and twistor methods in space-time geometry*. Cambridge University Press
- Percival W., *et al.*, 2001, *Mon.N.R.ast.Soc.*, **327**, 1297
- Perlmutter S., *et al.*, 1999, *Astrophys.J.*, **517**, 565
- Randall L., Sundrum R., 1999, *Phys.Rev.Lett.*, **83**, 4690
- Slosar A., *et al.*, 2002, *Cosmological parameter estimation and Bayesian model comparison using VSA data*, Submitted to *Mon.Not.R.astr.Soc.*, astro-ph/0212497
- Wareham R., Lasenby J., Lasenby A., 2003, *Computer graphics using Conformal Geometric Algebra*, To appear in *Phil.Trans.R.Soc.London.A*